Electrochemical and Optical Behavior of 8-Hydroxypyrene-1,3,6-trisulfonic Acid at Optically Transparent Electrodes

Ronnee N. Andrews,[a,b] *Carl J. Seliskar*,[b] *William R. Heineman*[b]*

[a] National Institute for Occupational Safety and Health, Centers for Disease Control and Prevention, U.S. Department of Health and Human Services, Cincinnati, Ohio 45226, USA
[b] Department of Chemistry, University of Cincinnati, 301 Clifton Court, Cincinnati, Ohio, 45221-0172, USA
fax: (513)556-9239
*e-mail: william.heineman@uc.edu

Received: December 2, 2009
Accepted: January 11, 2010

Abstract
The objective of this work is to elucidate the electrochemical and corresponding optical properties of 8-hydroxypyrene-1,3,6-trisulfonic acid (HPTS), using optically transparent electrodes, thereby deducing its usefulness as a model compound for spectroelectrochemical sensor development. Three pH levels were tested to determine optimal solution conditions for optical signal modulation. The electrolysis of HPTS follows an ECE mechanism, presumably resulting in the formation of a dihydroxy/dione derivative, and modulates the optical response at 405 and 460 nm wavelengths for pH 5 solutions. HPTS is a good candidate for spectroelectrochemical sensor research.

Keywords: 8-Hydroxypyrene-1,3,6-trisulfonic acid, HPTS, Cyclic voltammetry, Optically transparent electrodes, Absorbance, Sensors

DOI: 10.1002/elan.200900588

1. Introduction

Spectroelectrochemical sensors use both the optical and electrochemical properties of an analyte to achieve selectivity. The spectroelectrochemical sensor design has been described in detail elsewhere [1–5]. Briefly, the sensor utilizes optical modulation caused by cycling between two oxidation states that are characteristically different in their optical properties for quantification. Additional selectivity and sensitivity are provided by a charge selective polymer film that both selectively partitions and preconcentrates the analyte of interest. Model analytes used include: $Fe(CN)_6^{4-/3-}$, $Ru(BiPy)_3^{2+/3+}$, and $Ru(CN)_6^{3-/4-}$. These analytes undergo reversible electrolysis and optical modulation based upon oxidation state. Any analyte used with this sensor design must be shown to modulate optical signal through changes in oxidation state.

A previous application for this sensor was ferrocyanide detection in radioactive waste tanks [6] and, in an effort to expand its applicability, other potential model compounds are currently being investigated. One such compound is 8-hydroxypyrene-1,3,6-trisulfonic acid (HPTS). HPTS is classified by the FDA for use in externally applied drugs and cosmetics; however, its concentration may not exceed 0.01% by weight of the final drug or cosmetic product [7]. Due to these limitations, a sensor for HPTS would be valuable for the manufacturing and quality control aspects of this industry. HPTS may also prove valuable in preliminary development of a sensor for polyaromatic hydrocarbons (PAHs). Typically, PAHs are monitored using a biomarker and 1-hydroxypyrene (1-OHP) commonly fills that role [8–16]. Due to its toxicity and low water solubility, 1-OHP is not necessarily the best candidate for preliminary research in this area. However, because of its similar structure and pK_a to 1-OHP, HPTS is an excellent substitute for preliminary research on a 1-OHP spectroelectrochemical sensor.

HPTS is a non-toxic photoacid [17] with ground state pK_a values ranging from 7.3–8.1 [18, 19], and its excited state pK_a has been reported as both 0.32 [20] and 1.4 [19, 21]. It is widely used in probes of proton transfer kinetics [20, 22–29]. HPTS has high water solubility, large quantum yield, and Stokes' shift [18]. The wavelength of maximum absorbance and the excitation wavelength for emission are strongly dependent upon pH, while the emission wavelength is not and is consistently ca. 511 nm [19]. In alkaline solutions, an absorption band around 460 nm is present; however, this band disappears as the solution becomes more acidic and a peak at 405 nm forms. While the photooxidation of HPTS has been shown to form radical cations that may react with other phenols in solution to partially recover HPTS [30, 31], only limited information addressing the electrochemical properties of HPTS could be found in the literature [32, 33]. In these works, the oxidation of HPTS is stated to occur at 0.42 V (vs. the saturated calomel electrode) in alkaline solutions and

0.45 V (no reference electrode listed) under neutral conditions and was described as monoelectronic. Few other details were reported.

Preliminary experiments have determined that HPTS is electroactive at several working electrodes, including Au disk, Pt disk, glassy carbon disk, and at the optically transparent indium tin oxide (ITO) electrode [34]. While, the electrode material must be optically transparent for use in a spectroelectrochemical sensor, the electrochemical response of HPTS at the disk electrodes is improved over that at the ITO electrode. As shown by Zudans, et al. [35], however, hybrid working electrodes, composed of a thin metal layer on an optically transparent support, acquire a surface material more appropriate for the electrolysis of the analyte with minimal reduction in the optical transparency of the electrode. The durability of these electrodes can be improved, due to improved adhesion, with the use of ITO as the base of the electrode instead of glass [36].

In order to use HPTS as a model compound for spectroelectrochemical sensor development, it must be found to electrochemically modulate its absorbance response. Therefore, the aim of this work is to report the electrochemical characteristics, and corresponding optical response, of HPTS in aqueous solutions of varying pH at optically transparent electrodes. Indium tin oxide (ITO) and hybrid Au-sputtered ITO (Au-ITO) electrodes were compared as appropriate working electrodes. This study is the necessary initial step in deducing the usefulness of HPTS as a model compound for the development of a spectroelectrochemical sensor.

2. Experimental

2.1. Materials

Acetic acid (Pharmco Reagent Grade), sodium acetate, potassium nitrate, sodium phosphate dibasic anhydrous, sodium tetraborate, (all from Fisher), potassium phosphate monobasic (Baker Analyzed Reagent), hydroxypyrene trisulfonic acid trisodium salt (Molecular Probes or Sigma) and ethanol (Aaper Alcohol and Chemical Co.) were used without further purification. The pH 5 buffer was composed of 0.15 M sodium acetate and 0.15 M acetic acid. The pH 7 buffer was prepared with 0.076 M sodium phosphate dibasic anhydrous, 0.076 M potassium phosphate monobasic. The pH 9 buffer was composed of 0.067 M Borax. Either 0.1 or 1 M KNO_3 was used as the supporting electrolyte. All solutions were prepared with $>17\,M\Omega$ deionized water (Barnstead Nanopure system). Indium tin oxide (ITO) electrodes were obtained from Thin Film Devices, where ITO was coated onto a base of 1.1 mm thick 1×4 cm Corning 1737F glass (150 ± 10 nm, 20 Ω/sq.). Hybrid optically transparent electrodes were prepared on ITO electrodes. For hybrid electrode preparation, ITO electrodes were scrubbed with Neutrad solution, rinsed with alternating amounts of ethanol and deionized water, and exposed to argon plasma for at least 30 min. Au was sputter-coated onto the ITO electrode using a Denton Vacuum Sputter Coater at 50 mTorr and 45 mA. Gold film thicknesses deposited under these conditions were previously measured using ellipsometry and estimated to deposit at a rate of 0.33 nm/s. Therefore, a 10 nm layer of Au required 30 s of exposure. After sputter-coating, the Au-ITO electrodes were annealed in a Thermodyne muffle furnace at 280 °C for 2 h and allowed to cool overnight in the closed furnace. The assembly of optically transparent thin layer electrodes (OTTLE) followed an established procedure [36], with slight modifications: a glass microscope slide was used instead of a second electrode and the arrangement of the silicone sheeting was altered [34]. The OTTLE was composed of 0.010 in. thick strips of silicone sheeting sandwiched as a spacer between an optically transparent working electrode (either ITO or 10 nm thick Au-ITO) and a glass microscope slide. Cell volume was approximately 30 μL. In order to allow for electrode connection to the potentiostat, the glass slide was approximately 1 cm shorter than the electrode. The strips of silicone sheeting were arranged with a small gap at the top to allow for the cell to be filled through capillary action from the bottom.

2.2. Procedure

Measurements were made using a standard electrochemical workstation (either Bioanalytical Systems BASi Epsilon-EC or BAS 100W). A Au-ITO working electrode, platinum mesh auxiliary electrode and a Ag/AgCl, 3 M NaCl reference electrode from BAS were used in the scan rate study. The OTTLE was used for all other electrochemical experiments, along with a platinum wire auxiliary electrode, a miniature Ag/AgCl, saturated KCl reference electrode, and either a Au-ITO or ITO electrode. Absorbance spectra were recorded intermittently using a Cary 50 Bio UV-Visible Spectrophotometer blanked to air.

3. Results and Discussion

3.1. Cyclic Voltammetry-Bulk Solution

Cyclic voltammograms of a 3.77 mM HPTS solution (pH 5) at the 10 nm Au-ITO electrode were obtained at different scan rates: 1, 5, 10, 20, 40, 80, 100, and 200 mV/s. For each scan rate, a fresh aliquot of HPTS solution was used and three cycles were completed. The resulting CVs for three of the scan rates measured (10, 40, and 100 mV/s) are shown in Figure 1. Well defined anodic and cathodic peaks (designated I in Fig. 1), located at 0.64 and 0.52 V, respectively, are observed in bulk solution, corresponding to electrolysis of parent HPTS. At slower scan rates (1 to 40 mV/s), a second redox couple (designated II) is observed at 0.16 V. Peak II only appears after the oxidation of HPTS. While the peak current of the initial redox couple decreases in magnitude with each successive cycle, peak current increases in magnitude with cycling for peak II.

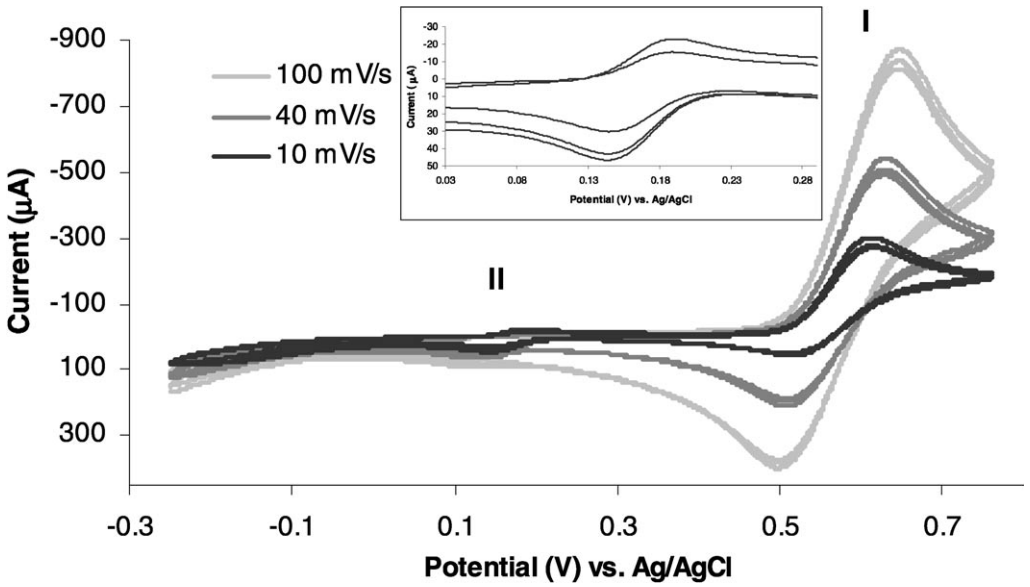

Fig. 1. Cyclic voltammograms of 3.77 mM HPTS/0.1 M KNO_3 at varying scan rates. 10 nm Au-ITO working electrode, Pt wire auxiliary electrode, Ag/AgCl reference electrode. Inset contains magnified CV response of the peak II couple at 10 mV/s.

The average peak current ratios as a function of scan rate are shown in Figure 2. For the 40 mV/s scan rate, the peak II couple does not appear until the second cycle and, therefore, the result shown is due to only 1 measurement, and not an average. For the peak I couple, the peak current ratio decreases with increasing scan rate, whereas the opposite occurs for the peak II couple: Up to a scan rate of 40 mV/s, the peak current ratio increases with increasing scan rate.

Based upon the formation of peak II at slower scan rates and the dependence of the peak current ratio to the scan rate, it appears that the electrolysis of HPTS follows an ECE mechanism. The decrease in current response for peak I while current increases for the peak II couple indicates that the parent HPTS is depleted by the generation of a new product. Therefore, the two couples are linked. The decrease in peak current ratio with increasing scan rate for peak I also indicates that electrolysis of parent HPTS follows an EC mechanism with a reversible electrochemical step followed by a chemical step [37]. The relationship of anodic to cathodic peak current ratio for the peak II couple indicates electrolysis with a preceding chemical reaction (CE mechanism) [37]. Therefore, the chemical step of the parent HPTS electrolysis is the chemical step preceding the electrolysis of the second redox couple (peak II), and the overall mechanism is ECE. At slower scan rates, the chemical reaction proceeds, resulting in the second redox couple. However, scan rates greater than 40 mV/s are sufficiently quick to outrun the chemical reaction and peak II does not appear. This is typical behavior of the ECE mechanism.

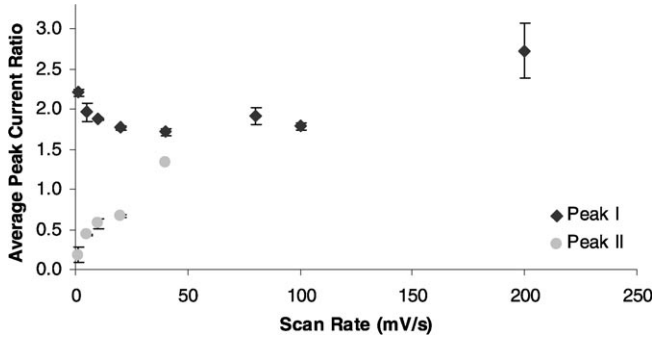

Fig. 2. Average peak current ratio ($N=3$ for peak I couple and $N=2$ for peak II couple) as a function of scan rate for 3.77 mM HPTS in pH 5 buffer solutions with 0.1 M KNO_3 at 10 nm Au-ITO. Error bars ± standard deviation.

3.2. Electrochemistry at the OTTLE

Both ITO and Au-ITO were examined as possible working electrodes in OTTLE experiments. While the electrochemical response of HPTS at ITO is less than ideal for bulk solutions, the considerably slower scan rate used in thin layer CV improves the electrolysis at ITO. With the ultimate goal as the development of a spectroelectrochemical sensor that relies upon a modulation of optical signal for detection, ideal electrochemical response is not critical; what is critical is that the electrolysis elicits a (preferably) reversible change in the optical response. CVs of HPTS solutions at pH 5, 7, and 9 were obtained at both the Au-ITO and ITO OTTLE (Fig. 3). All CVs were recorded within the available potential window for the specific pH/working electrode combinations and commenced at the rest potential. Rest potentials range from 0.043 to 0.220 V (vs. Ag/AgCl).

The resulting CV waves appear distorted with large peak potential differences and broad waves due to IR drop. In the OTTLE set-up, the electrical contacts are at the top of the working electrode. Therefore, the current must travel the

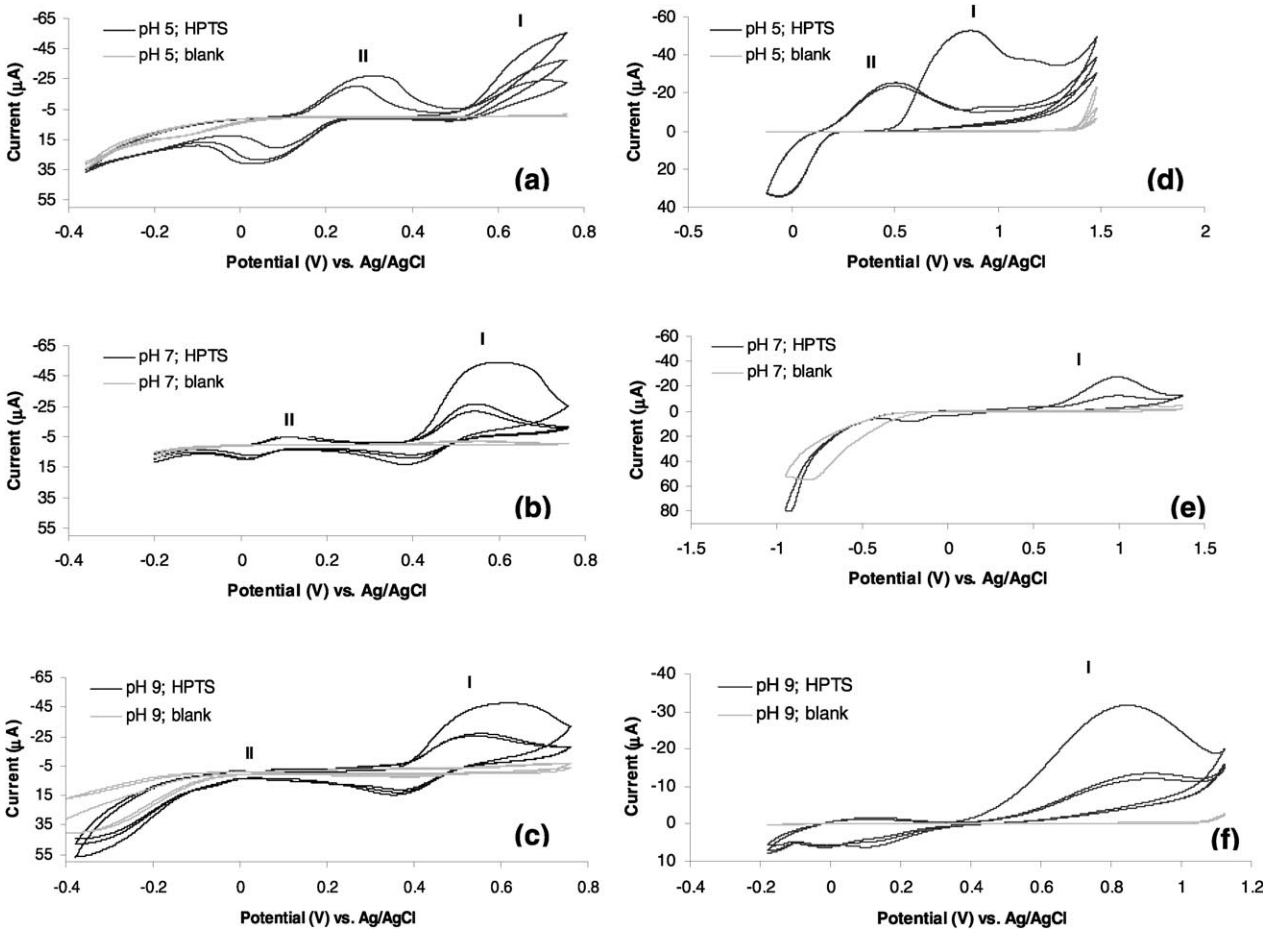

Fig. 3. Cyclic voltammograms of 4 mM HPTS/0.1 M KNO_3 solutions at the (a – c) 10 nm Au-ITO and (d – f) ITO OTTLE cells for 3 pH levels. 1 mV/s scan rate.

relatively expansive length of the working electrode and resistance increases. The OTTLE design is also plagued by increased solution resistance that requires concentrations of supporting electrolyte larger than that required for conventional cells with of semi-infinite diffusion. The concentration of supporting electrolyte (0.1 M) used for the pH study is not sufficient to diminish the effect of resistance. As confirmation of solution resistance as a source of CV peak distortion, CV peak shape improves with increased supporting electrolyte concentrations (results not shown).

At the Au-ITO OTTLE, the results are similar to that of the bulk solution at Au-ITO: the anodic peak of the peak I couple (0.76 V at pH 5, 0.59 V at pH 7, and 0.62 V at pH 9) greatly diminishes after the first cycle, and continues to decrease with subsequent cycles, and a second redox couple (peak II) forms, which increases in peak current with continued cycling of the applied potential. At pH 5, the cathodic peak of the peak I couple is absent. At pH 7 and pH 9, the cathodic peak is present, albeit at much lower peak height than that of the corresponding anodic peak. The second redox couple is absent if the potential is not first scanned sufficiently positive to oxidize the parent HPTS solution. In general, a decrease in the pH of the solution results in an increase in the response of the peak II couple, such that the electrochemical response of the second redox couple is greatest for pH 5 solutions. The CV response negative of -0.11 V is present in the blank and is not due to HPTS electrolysis.

At the very slow scan rate required of thin layer experiments, electrolysis of HPTS is possible at ITO surfaces. At 1 mV/s, the slow electron transfer kinetics at the ITO electrode are on the time scale of the electrochemical experiment. As with HPTS electrolysis at the Au-ITO OTTLE, the anodic peak due to parent HPTS (peak I) decreases with cycling at each pH value at ITO surfaces. At no pH level is the corresponding cathodic peak detected. The CV of pH 5 solutions at ITO most closely resembles the electrolysis of HPTS at Au-ITO: a second redox couple (peak II) forms only after the initial HPTS oxidation at less positive potentials than the first couple (peak I). At ITO, the peak II couple is of near constant magnitude over 3 cycles. The CV response at potentials less than -0.4 V is due to blank electrolysis.

For both Au-ITO and ITO working electrodes, the anodic peak potential is most positive for HPTS in pH 5 solutions and occurs at less positive potentials in pH 7 and pH 9 solutions. This behavior indicates that oxidation is facilitated by deprotonation of HPTS and which is not uncom-

mon in the oxidation of organic compounds [38]. HPTS is mostly protonated at pH 5 and mostly deprotonated at pH 9. Thus, the oxidation of HPTS is more difficult at the lower pH level (pH 5), where HPTS is protonated, and occurs at a more positive potential.

The thin layer results support the bulk solution finding that the electrolysis of HPTS is due to an ECE mechanism. Decreased availability of HPTS after the first scan and the formation of a second redox couple are indicative of ECE. Because the second redox couple only forms after parent HPTS oxidation, the connection of the initial oxidation to the new couple is clear. The apparent irreversibility of parent HPTS electrolysis is due to the scan rate used in these OTTLE experiments; the 1 mV/s scan rate used is sufficiently slow to allow for the chemical reaction that follows HPTS oxidation to occur. Thus, the cathodic peak corresponding to the parent HPTS oxidation is not present or present at such relatively small currents to indicate irreversibility. Another complicating factor is that the oxidation of HPTS has been shown to form radicals that may react to partially recover HPTS [31]. This could explain why the HPTS is not completely depleted with potential cycling.

Due to the resemblance of the CVs of thin layers of HPTS to that shown for thin layers of 1-OHP [39, 40], the sulfonate groups of HPTS do not appear to substantially affect HPTS electrolysis. Therefore, the products of HPTS electrolysis in acidic aqueous solutions should be of similar structure to the oxidation products of 1-OHP. The final oxidation products of 1-OHP have been identified as dihydroxypyrene and pyrenedione [39 – 44] and, thus, the second redox couple in the CVs of HPTS may be identified as a dihydroxy/dione derivative of HPTS. Peak I is assigned as the oxidation of parent HPTS, which results in the formation of radical ions, and peak II couple as the dihydroxy/dione derivative. The electrolysis potentials for HPTS are slightly shifted from those found by Mazur, et al. [40] for adsorbed 1-OHP. These differences may have resulted from the large resistance inherent to the OTTLE (as described above), as well as the presence of the sulfonate groups and the difference between an adsorbed species and a dissolved species.

While the newly formed product is stable for the duration of the CV experiments, it does not possess long-term stability. After 5 days of storage, the CV analysis of an electrolyzed solution of HPTS in a pH 5 buffer at the Au-ITO OTTLE shows an order of magnitude loss in peak current. The generation of HPTS radicals may be responsible for the limited stability of the generated product. The stability issues, along with the incomplete conversion of parent HPTS to the new product, hindered attempts to elucidate the structure of the electrolysis product with mass spectrometry and NMR. Results from these analyses are inconclusive.

Based upon the CV results, the electrolysis of HPTS is best at the Au-ITO electrode. For the 3 pH levels tested, 2 couples are consistently detected at Au-ITO, while it is only at pH 5 that the second couple forms at the ITO electrode. Also, the large resistance inherent to ITO electrodes, though partially overcome with the use of a slow scan rate, causes peak current suppression and increased peak potential differences. There are limitations in the use of the Au-ITO electrodes. First, the Au coating is sensitive to the applied potential, with a Au oxide layer forming that obscures HPTS electrolysis response if a potential is applied beyond 0.76 V (vs. Ag/AgCl). Also, the Au coating is sensitive to touch and can be removed from the electrode with a slight wipe of its surface.

3.3. Spectroelectrochemistry at the OTTLE

In order to establish the conditions for the determination of HPTS by electrochemically modulated optical signals, thin layer spectroelectrochemical spectra were obtained by sequential controlled potential electrolysis (CPE) experiments of 4.04 mM HPTS/1.01 M KNO_3 in pH 5 solution at the Au-ITO OTTLE. Potentials were held at 0.76 V for 7 min, – 0.36 V for 19 min, 0.45 V for 13.5 min, and, finally, at 0.76 V for 10 min. Potentials were chosen at values beyond the electrolysis potentials, if possible, and hold times were based on the time required to achieve that potential if a scan rate of 1 mV/s were used. In order to capture the effect of potential on absorbance response, absorbance spectra were recorded every 3 min. Figure 4 shows the average ($N = 4$) absorbance spectrum at each potential.

A modulation of the optical response occurs with variation in the potential applied. Initially, no peak is present at 460 nm; however, after the potential is held at 0.76 V (and parent HPTS is subsequently oxidized), a peak at 460 nm grows in and the absorbance response increases by 0.5 a.u. The signal then drops to near-baseline levels when the potential is switched to – 0.36 V. At this potential, the electrogenerated product (peak II) is reduced. Next, the peak at 460 nm again grows in after the potential is held at 0.45 V, a potential just positive of the anodic peak potential of the peak II species, and the absorbance modulation at 460 nm is approximately half of the initial increase. At the final 0.76 V hold, the absorbance increases to 1.0 a.u. (0.1 a.u. above the response of the initial 0.76 V hold). The absorbance at 405 nm remains relatively constant through-

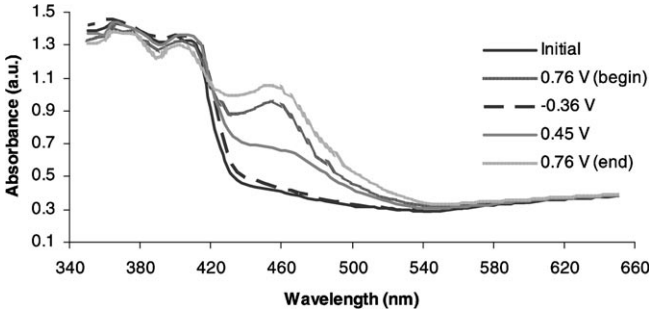

Fig. 4. Average ($n = 4$) absorbance spectra of 3.97 mM HPTS/ 1.03 M KNO_3 in pH 5 solutions at the Au-ITO OTTLE cell during CPE. Displayed spectra were recorded at the end of the hold time for each potential (vs. Ag/AgCl).

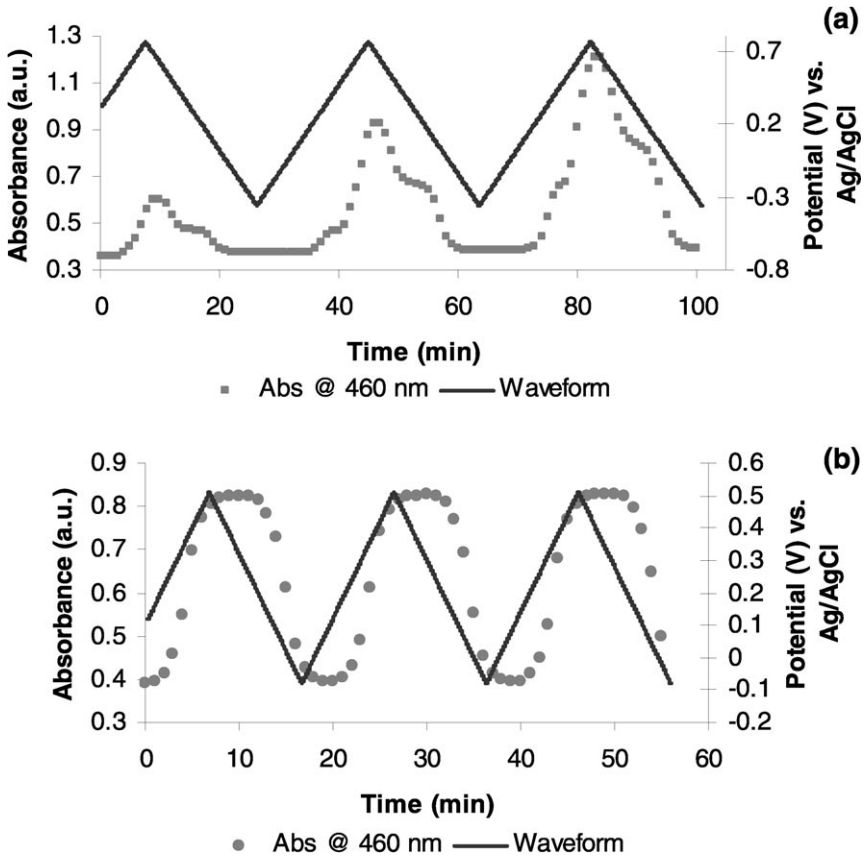

Fig. 5. Optical response of 4 mM HPTS/0.1 M KNO_3 in pH 5 solutions at the Au-ITO OTTLE while cycling applied potential (a) within the entire potential window and (b) within the potential window of the generated species and the applied waveform. 1 mV/s scan rate.

out the experiment, but decreases slightly during the final 0.76 V hold that reoxidizes the solution components.

The absorbance of HPTS solutions at Au-ITO or ITO OTTLE was recorded intermittently as CVs were performed at 1 mV/s. (The corresponding CVs are displayed in Fig. 3.) While the absorption spectra were recorded over 350 – 650 nm, the wavelengths focused upon for modulation include 405 and 460 nm only. It is at these wavelengths that changes in the absorption spectrum occur due to the protonation state of the parent HPTS molecule. The maximum absorbance for protonated HPTS occurs at 405 nm; however, when it is deprotonated, the maximum response shifts to 460 nm. When both protonated and deprotonated HPTS are in solution, absorbance occurs at both wavelengths. The absorbance spectra recorded using the OTTLE show similar relationships to solution pH. Also, a measured change at 460 nm occurred with HPTS electrolysis in the CPE experiment (Fig. 4). Thus, the optical responses shown with the imposed CV waveform include data at 405 and/or 460 nm only.

As shown in Figure 5, absorbance modulates with applied potential for pH 5 solutions at Au-ITO OTTLE. During oxidation, the absorbance response at 460 nm increases and, during the reduction step, returns to baseline at the Au-ITO OTTLE. The magnitude of the modulation at 460 nm increases with time (successive oxidations) from 0.2 to 0.8 a.u. The absorbance response at 405 nm does not modulate with applied potential for HPTS in a pH 5 solution at Au-ITO OTTLE. The pH 5 blank absorbance response at Au-ITO OTTLE is also constant with an absorbance of 0.3 a.u. at both 405 and 460 nm.

Absorbance modulations at Au-ITO OTTLE vary in shape when the potential is cycled within the entire available potential window and when it is cycled only within that for the second redox couple. For the full window (Fig. 5a), the modulation at 460 nm appears to have shoulders at the leading and tailing edges; however, the modulation of the new couple, as shown in Figure 5b, simply plateaus at a lesser absorbance magnitude. Also, the modulations of the new couple are of consistent magnitude, while those for cycles within the full potential window do not display such reversibility.

As with Au-ITO, modulation of the absorbance response occurs at ITO OTTLE (Fig. 6). The absorbance response at 460 nm at the ITO OTTLE increases during oxidation, and the response decreases during the reduction step for HPTS in pH 5 solutions. The first modulation is 0.4 a.u. and decreases to 0.2 a.u. for the second and third modulations. The absorbance modulation at 405 nm is the mirror image of the response at 460 nm for the ITO OTTLE: absorbance at 405 nm increases during the reduction segment and decreases during the oxidation segment. The 405 nm modu-

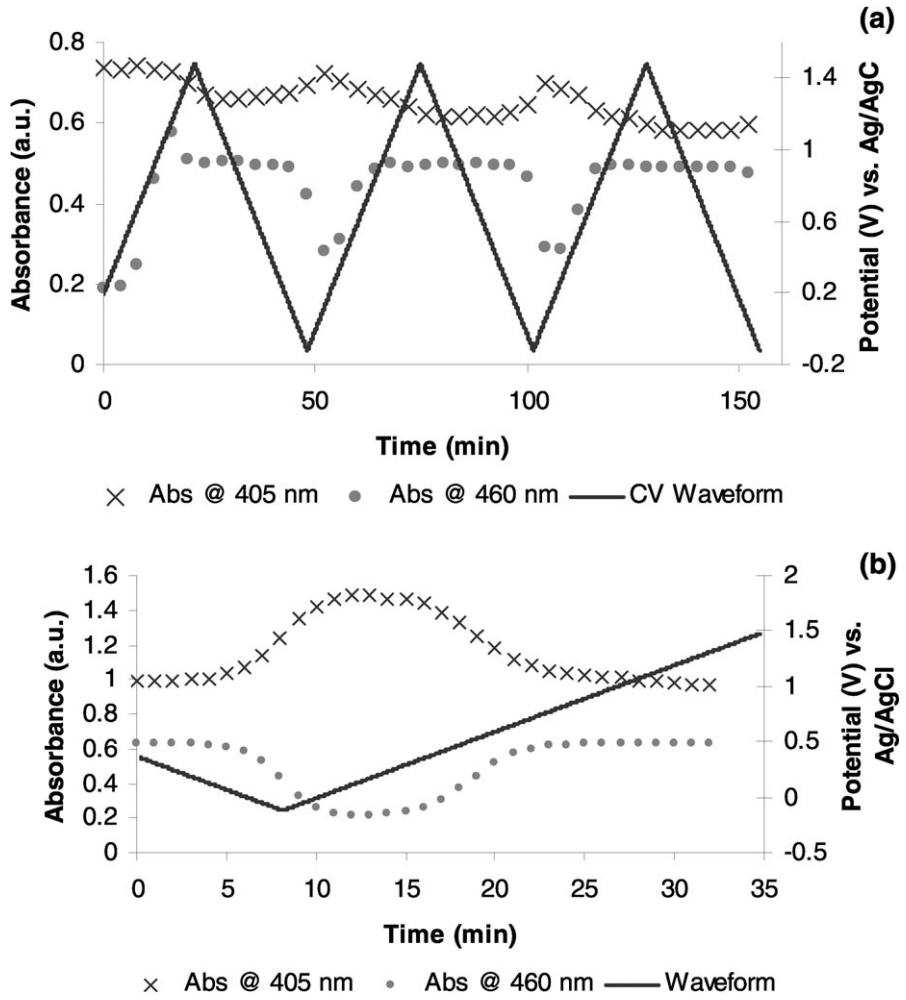

Fig. 6. Optical response of 4 mM HPTS/0.1 M KNO_3 in pH 5 solutions at the ITO OTTLE while cycling applied potential (a) within the entire potential window and (b) within the potential window of the generated species and the applied waveform. 1 mV/s scan rate.

lation is only 0.1 a.u. in magnitude. The overall absorbance response at 405 nm decreases over the course of the experiment at the ITO OTTLE. The blank absorbance response at both 405 and 460 nm is constant at 0.2 a.u. over the course of the experiment.

When the potential cycles within that for parent HPTS electrolysis only (peak I couple), the absorbance response at ITO becomes steady at both 405 and 460 nm, after the initial oxidation and absorbance change. Afterwards, the absorbance is able to modulate as the generated species (peak II) is electrolyzed. Within this smaller potential window, as shown in Figure 6b, the 460 nm response reaches a minimum when the species is in its reduced state and a maximum when in its oxidized state. As with the full potential window, the response at 405 nm is the mirror image of that at 460 nm when the potential cycles solely within that of the peak II couple.

Absorbance modulations are visible for pH 7 solutions at Au-ITO; however, they lack the definition shown for pH 5 solutions. The increase in 460 nm absorbance is greatest for the initial oxidation (approximately 0.2 a.u.). The modulations then decrease drastically to < 0.05 a.u. and shift to less positive potentials for subsequent cycles. Absorbance at 405 nm does not change during the CV for the full potential window; but, during the CV of the peak II couple, it varies without any apparent pattern or relation to the applied potential. Absorbance at 460 nm is stable when the potential cycles only within the window for the peak II couple. No absorbance change related with cycled potential is evident at the ITO OTTLE for pH 7 solutions. Solutions of pH 7 at ITO OTTLE show no change in the absorbance at 405 nm and an increase in absorbance signal at 460 nm of 0.3 a.u. during the beginning of the initial oxidation segment. Then, the response begins to decrease to baseline before the applied potential reaches the switching potential. The blank pH 7 absorbance response does not modulate at either the Au-ITO or ITO OTTLE.

For pH 9 solutions at the Au-ITO OTTLE, the 460 nm absorbance initially remains steady, but begins to increase in magnitude by 0.4 a.u. around the switching potential. After the next oxidation segment, the response drops and continues to decline over the course of the experiment. The 405 nm response increases during the initial oxidation segment, reaching its maximum absorbance during oxida-

tion with a 1.1 a.u. modulation. After the initial increase, the absorbance at 405 nm continues to gradually increase with time. Potential application to pH 9 solutions at the ITO OTTLE results in a 1 a.u. increase in absorbance at 405 nm, as shown in Figure 7. Very slight absorbance increases occur at the oxidation switching potentials of the next 2 cycles. The response at 460 nm decreases by 1.3 a.u. with the initial oxidation step and continues to decline over the course of the experiment in a step-wise fashion. Spectral etaloning is evident in the initial absorption spectrum for pH 9 solutions at the ITO OTTLE. No modulation occurs using the blank pH 9 solutions at either the Au-ITO or ITO OTTLE; however, at the Au-ITO OTTLE, the blank absorbance (at both 405 and 460 nm) increases by approximately 0.2 a.u. over the course of the experiment.

As expected, the initial wavelength of maximum absorption of HPTS solution depends upon the pH of the solution: Under acidic conditions, 405 nm is the wavelength of maximum absorption and, under basic conditions, 460 nm is maximum. The pK_a of HPTS is in the range of 7.3 – 8.1 [18, 19]; therefore, in a pH 5 solution, the majority of HPTS in solution is protonated. It follows that the absorption of protonated HPTS (405 nm) would be greater than that of deprotonated HPTS (460 nm), as is shown. For pH 9 solutions, where HPTS is initially deprotonated, the converse is shown: Absorbance at 460 nm is greater than that at 405 nm. For pH 7, both protonated and deprotonated HPTS are present in solution, thus measurable absorbance responses are detected at both 405 and 460 nm.

Based upon CPE and CV experiments on pH 5 solutions, the modulated responses are due to both the electrolysis of the parent HPTS and that of the generated compound. The initial change in absorbance response is due to the oxidation of parent HPTS. As HPTS is depleted in solution, the portion of the absorbance due to its electrolysis decreases. The oxidation of the generated species results in absorbance changes similar to that shown for parent HPTS, albeit to a lesser magnitude; therefore, subsequent optical modulations are due to a combination of the parent HPTS and its electrogenerated derivative. For parent HPTS oxidation at ITO, the absorbance response stabilizes after the first oxidation segment, so the succeeding modulations are due to the electrogenerated species.

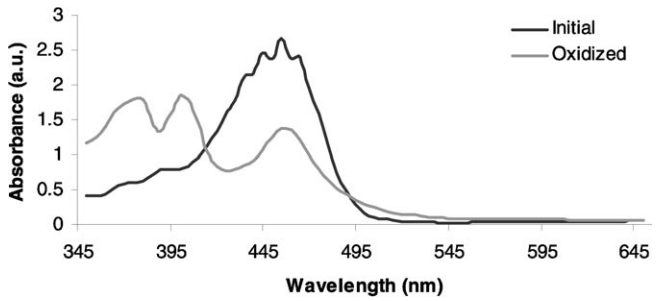

Fig. 7. Absorbance spectra of 4 mM HPTS/0.1 M KNO_3 in pH 9 solution at ITO OTTLE before potential application and after the oxidation segment of CV

Two options exist for a spectroelectrochemical sensor for HPTS. First, with pH 5 solutions, the absorbance modulations that occur throughout the CV can be used for HPTS determination. Due to the multiplicity of the modulations, either a single modulation or the average of the modulations could be related to HPTS concentration. The other option is to use absorbance change due to the first oxidation segment of pH 9 solutions.

Based upon absorbance modulation results, ITO electrode is a better choice for the working electrode. For pH 5 solutions, there is less variation in the magnitude of the absorbance modulations at ITO, which allows for the possibility of signal averaging. Due to the nature of the experiment, where absorption spectra were recorded intermittently based upon time lapsed and not upon the potential applied, some variation in the magnitude of the modulations is expected. However, the degree to which the modulations varied at Au-ITO OTTLE can not be attributed solely to experimental design. Also, the ITO electrode offers improved selectivity due the absorbance response modulating at two wavelengths (405 or 460 nm); therefore, either wavelength may be monitored and used for detection. While larger modulations occur for pH 5 solutions with Au-ITO than with ITO, the potential surface changes of the Au-ITO electrode complicate the relationship of absorbance modulation to analyte electrolysis, thereby complicating the detection scheme. For low level detection of HPTS, pH 9 solutions should be used. While only a single measurement may be recorded (relating to the oxidation of parent HPTS) for each system, the absorbance modulation for pH 9 solutions is twice that for pH 5 solutions with Au-ITO and, depending upon the wavelength monitored, 3 or 9 times that for pH 5 solutions with ITO.

4. Conclusions

Although HPTS electrolysis is more ideal at Au-ITO electrodes, it is electroactive at both Au-ITO and ITO electrodes. The oxidation of HPTS results in deprotonation of HPTS and, after a chemical reaction, the formation of a new redox couple, which is presumably its dihydroxy/dione derivative. This ECE mechanism is most apparent for acidic solutions. The absorbance response modulates with applied potential, and, depending upon solution pH, the modulations are due to both the electrolysis of parent HPTS and its newly formed redox species (pH 5) or only parent HPTS oxidation (pH 9). Absorbance modulations at ITO offer improved sensitivity and selectivity over those at Au-ITO. The choice of solution pH and electrode should take into consideration the analytical application. For electrochemical detection, Au-ITO electrodes offer improved CV response and are preferred over ITO electrodes; however, for an absorbance-based spectroelectrochemical sensor, the ability to modulate the optical response through application of potential is essential, and ITO electrodes are preferred over Au-ITO electrodes. Overall, HPTS is a good candidate for spectroelectrochemical sensing and this detection

scheme may prove valuable if an appropriate detection limit can be obtained for a given application.

Acknowledgements

The authors gratefully acknowledge support from the *Office of Science (BER)*, *U.S. Department of Energy*, Grant No. DE-FG02-07ER64353. The authors also thank Dr. *Nebojsa Pantelic* for his work on the measurement of sputter-coated Au film thicknesses. RNA thanks the *National Institute for Occupational Safety and Health* Long-Term Training Program for the opportunity to work on this project.

Disclaimer: The mention of company names does not constitute endorsement by the Centers for Disease Control and Prevention.

References

[1] Y. Shi, C. J. Seliskar, W. R. Heineman, *Anal. Chem.* **1997**, *69*, 4819.
[2] Y. Shi, A. F. Slaterbeck, C. J. Seliskar, W. R. Heineman, *Anal. Chem.* **1997**, *69*, 3679.
[3] A. Slaterbeck, T. H. Ridgway, C. J. Seliskar, W. R. Heineman, *Anal. Chem.* **1999**, *71*, 1196.
[4] M. Maizels, C. J. Seliskar, W. R. Heineman, *Electroanalysis* **2000**, *12*, 1356.
[5] W. R. Heineman, C. J. Seliskar, J. N. Richardson, *Russ. J. Electrochem.* **2003**, *39*, 982.
[6] M. L. Stegemiller, W. R. Heineman, C. J. Seliskar, T. H. Ridgway, S. A. Bryan, T. Hubler, R. L. Sell, *Environ. Sci. Technol.* **2003**, *37*, 123.
[7] FDA, *Color Additive Status List*, U.S. Department of Health and Human Services, Food and Drug Administration, Center for Food Safety and Applied Nutrition, College Park, MD **2007**; [http://www.cfsan.fda.gov/~dms/opa-appc.html]. Date accessed: October **2008**.
[8] W. P. Tolos, P. B. Shaw, L. K. Lowry, B. A. MacKenzie, J.-F. Deng, H. L. Markel, *Appl. Occup. Environ. Hyg.* **1990**, *5*, 303.
[9] F. J. Jongeneelen, *Sci. Total Environ.* **1997**, *199*, 141.
[10] M. Bouchard, K. Krishnan, C. Viau, *Toxicol. Sci.* **1998**, *46*, 11.
[11] M. Bouchard, C. Viau, *Biomarkers* **1999**, *4*, 159.
[12] F. J. Jongeneelen, *Ann. Occup. Hyg.* **2001**, *45*, 3.
[13] C.-E. Bostrom, P. Gerde, A. Hanberg, B. Jernstrom, C. Johansson, T. Kyrklund, A. Rannug, M. Tornqvist, K. Victorin, R. Westerholm, *Environ. Health Perspect.* **2002**, *110 S3*, 451.
[14] F. Jongeneelen, *J. Environ. Monit.* **2004**, *6*, 61N.
[15] J. Unwin, J. Cocker, E. Scobbie, H. Chambers, *Ann. Occup. Hyg.* **2006**, *50*, 395.
[16] ACGIH, in *Documentation of the Threshold Limit Values and Biological Exposure Indices, American Conference of Governmental Industrial Hygienists*, 7th ed., Cincinnati, OH **2008**, Suppl. 2002 – 2008.
[17] G. A. Lutty, *Toxicol. Appl. Pharmacol.* **1978**, *44*, 225.
[18] O. S. Wolfbeis, E. Furlinger, H. Kroneis, H. Marsoner, *Fresenius' J. Anal. Chem.* **1983**, *314*, 119.
[19] J. R. Lakowicz, in *Principles of Fluorescence Spectroscopy*, Springer, New York **1999**, pp. 548 – 549.
[20] M. J. Politi, J. H. Fendler, *J. Am. Chem. Soc.* **1984**, *106*, 265.
[21] R. Barnadas-Rodriguez, J. Estelrich, *J. Photochem. Photobiol. A* **2008**, *198*, 262.
[22] M. Gutman, D. Huppert, E. Pines, *J. Am. Chem. Soc.* **1981**, *103*, 3709.
[23] M. Gutman, D. Huppert, E. Nachliel, *Eur. J. Biochem.* **1982**, *121*, 637.
[24] M. J. Politi, H. Chaimovich, *J. Phys. Chem.* **1986**, *90*, 282.
[25] M. Gutman, E. Nachliel, S. Moshiach, *Biochemistry* **1989**, *28*, 2936.
[26] D. Roy, R. Karmakar, S. K. Mondal, K. Sahu, K. Bhattacharyya, *Chem. Phys. Lett.* **2004**, *399*, 147.
[27] R. Gepshtein, P. Leiderman, L. Genosar, D. Huppert, *J. Phys. Chem. A* **2005**, *109*, 9674.
[28] P. Leiderman, R. Gepshtein, A. Uritski, L. Genosar, D. Huppert, *J. Phys. Chem. A* **2006**, *110*, 5573.
[29] D. B. Spry, A. Goun, M. D. Fayer, *J. Phys. Chem. A* **2007**, *111*, 230.
[30] E. B. de Borba, C. L. C. Amaral, M. J. Politi, R. Villalobos, M. S. Baptista, *Langmuir* **2000**, *16*, 5900.
[31] C. Aliaga, A. Arenas, A. Aspee, C. Lopez-Alarcon, E. A. Lissi, *Helv. Chim. Acta* **2007**, *90*, 2009.
[32] C. Prayer, T.-H. Tran-Thi, S. Pommeret, P. d'Oliveira, P. Meynadier, *Chem. Phys. Lett.* **2000**, *323*, 467.
[33] P. P. Neelakandan, M. Hariharan, D. Ramaiah, *J. Am. Chem. Soc.* **2006**, *128*, 11334.
[34] R. N. Andrews, *Ph.D. Thesis*, University of Cincinnati, Cincinnati, OH **2009**.
[35] I. Zudans, J. R. Paddock, H. Kuramitz, A. T. Maghesi, C. M. Wansapura, S. D. Conklin, N. Kaval, T. Shtoyko, D. J. Monk, S. A. Bryan, T. L. Hubler, J. N. Richardson, C. J. Seliskar, W. R. Heineman, *J. Electroanal. Chem.* **2004**, *565*, 311.
[36] D. J. Monk, *Ph.D. Thesis*, University of Cincinnati, Cincinnati, OH **2003**.
[37] W. R. Heineman, P. T. Kissinger, in *Laboratory Techniques in Electroanalytical Chemistry*, 2nd ed. (Eds: P. T. Kissinger, W. R. Heineman), Marcel Dekker, New York **1996**, pp. 51 – 125.
[38] W. R. Heineman, in *Chemical Instrumentation: A Systematic Approach*, 3rd ed. (Eds: H. A. Strobel, W. R. Heineman), Wiley, New York **1989**, pp. 1055 – 1111.
[39] M. Mazur, G. J. Blanchard, *J. Phys. Chem. B* **2004**, *108*, 1038.
[40] M. Mazur, G. J. Blanchard, *Bioelectrochemistry* **2005**, *66*, 89.
[41] A. J. Fatiadi, *Environ. Sci. Technol.* **1967**, *1*, 570.
[42] Y. Mao, J. K. Thomas, *Langmuir* **1992**, *8*, 2501.
[43] M. E. Sigman, P. F. Schuler, M. M. Ghosh, R. T. Dabestani, *Environ. Sci. Technol.* **1998**, *32*, 3980.
[44] C. A. Reyes, M. Medina, C. Crespo-Hernandez, M. Z. Cedeno, R. Arce, O. Rosario, D. M. Steffenson, I. N. Ivanov, M. E. Sigman, and R. Dabestani, *Environ. Sci. Technol.* **2000**, *34*, 415.

